GEOFIZIKA VOL. 41 2024

DOI: https://doi.org/10.15233/gfz.2024.41.6
Original scientific paper

Utilizing remote sensing for monitoring land cover changes and land surface temperature fluctuations in Laos

Ketsana Phommavong and *Jianguo Yan*

State Key Laboratory of Information Engineering in Surveying, Mapping and Remote Sensing, Wuhan University, Wuhan, China

Received 15 December 2023, in final form 29 December 2024

Land cover change detection (*LCCD*) is essential for facilitating environmental conservation and sustainable development efforts around the world. This study examines the relationship between *LCCD* and land surface temperature (*LST*) in Thakhek, Laos, from 2000 to 2023. We evaluate the relationship between changes in land use patterns and land surface temperature (*LST*) variations using Landsat-5, Landsat-8, and Moderate Resolution Imaging Spectroradiometer (MODIS) datasets. Our results indicate a significant reduction in forest area, which decreases from 46,912 km^2 in 2000 to 33,955 km^2 in 2023, primarily due to human activities and rapid urbanization. At the same time, the barren area increased to 515.33 km^2, while the agricultural area decreased significantly to 2,975.97 km^2. The observed *LST* values show significant changes, ranging from 24 °C to 33 °C in 2000 and extending to 20 °C to 41 °C in 2023, indicating a general increase in temperature. The results illustrate the significant correlation between urban development, population growth, and land cover changes, which influence regional temperature trends in Thakhek. These results highlight the urgent need for targeted research and policy measures that combine development and environmental sustainability and ensure a harmonious regional future.

Keywords: land cover change, land surface temperature, Laos, urbanization, remote sensing

1. Introduction

Land use and land surface temperature (*LST*) are fundamental to understanding the interaction between human activities and environmental change. The rapid change in land cover due to urbanization, agriculture, and industrial development poses a major challenge to ecological stability and climate regulation. As populations grow and urban areas expand, the consequences of these changes are becoming increasingly evident, leading to changes in local climate, loss of biodiversity, and shifts in ecosystem services. Research has shown that changing land use can significantly affect on global and regional temperatures, as urban areas tend to exhibit the "urban heat island" effect, where temperatures are higher than in surrounding rural areas (Xu et al., 2021). This phenomenon is caused by factors such as reduced vegetation, larger impermeable surfaces, and heat-generating human activities.

In the study of the Thakhek district in Laos, the local government has pursued a land use policy over the past twenty-three years to convert forested and agricultural land into urban and industrial zones (Gogoi et al., 2019). This conversion has led to a significant increase in urban land cover, which contributes to temperature rise and changes in the climate dynamics of the region (Aram et al., 2019). Natural factors like forest fires and deforestation, along with infrastructure development, affect land cover and *LST* and play a crucial role in shaping land cover and influencing temperature patterns (Derdouri et al., 2021). The study was conducted by José Maria Cardoso da et al. (2017). Understanding these dynamics is crucial for effective environmental management and urban planning as land use is constantly evolving (Jin et al., 2009).

Remote sensing technologies have proven to be powerful tools for analyzing land cover change and its impact on *LST*. With these technologies, researchers can collect vast amounts of data over time, providing insight into spatial and temporal trends in land use. For example, Bucała (2014) used remote sensing to study the impact of human activities on the natural environment, highlighting the value of these technologies for environmental monitoring. Similarly, Mahmood et al. (2010) investigated the impact of land cover dynamics on summer climate and emphasized the need for comprehensive data for climate adaptation strategies.

In addition, to monitoring temperature changes, remote sensing has proven its worth in assessing the state of ecosystems and the effective management of resources. A study by Sruthi et al. (2015) looked into the connection between the normalized difference vegetation index (*NDVI*) and *LST*. The results showed how important vegetation is for keeping temperatures down and helping farming. The results of these studies emphasize the potential benefits of using remote sensing technologies to address pressing environmental issues, particularly in the context of sustainable land management.

The aim of this study is to investigate the relationship between *LST* and land cover change in the Thakhek district between 2000 and 2023. This work focuses on understanding how urbanization and industrialization affect local temperature patterns and whether the trends observed in other regions apply to this study. By clarifying these relationships, the aim of this research to gain valuable insights that can inform policymakers and stakeholders in their efforts to promote environmentally sustainable practices and enhance climate resilience in the region.

Through this research, the objective is to enhance our understanding of how land use changes impact land surface temperature (*LST*), emphasizing the importance of incorporating remote sensing data into environmental management strategies. Ultimately, the goal is to support informed decision-making processes that foster sustainable development in the Thakhek District and similar areas facing rapid land cover transformations.

2. Study area

This study is conducted in the Thakhek district of Laos (17°30'2.70" N, 104°53'49.17" E). Laos, a landlocked country in Southeast Asia, borders China to the north, Myanmar to the northwest, Thailand to the west and southwest, Vietnam to the east, and Cambodia to the south. The district of Thakhek covers an area of around 97,858 km^2 and includes a variety of landscapes, including forests, rivers, and agricultural land. Lao PDR covers an area of 236,800 km^2 and has a population of approximately 7.5 million with an annual growth rate of 2% (Cosslett and Cosslett, 2018). Demographic growth has a significant impact on land use and environmental change in the region. Assessing the topography and demographic patterns of the region is important to understand the impact of land cover changes and surface temperature variations in Thakhek district, especially with regard to urbanization and industrial growth (see Fig. 1).

3. Dataset and methodology

3.1. Dataset

The research employs satellite-imagery remote sensing data to analyze LST over several years. We have collected the data from MODIS, Landsat 4, 7, 8, and 9 satellite imagery from 2000, 2005, 2010, 2015, 2020, and 2023. Table 1 displays the summary data source. The estimation of *LST* during both daytime and nighttime is analyzed using MODIS data through Google Earth Engine. These datasets were acquired through the United States Geological Survey (USGS) Earth Resource Observation Data Center (ERODC) website (https://www.usgs.gov/). The approach was conducted with the geospatial tool ArcGIS 10.8 software in conjunction with Python analysis.

3.2. Methods

The study uses Landsat data and Python analysis techniques to estimate land cover change detection (*LCCD*) over periods 2000, 2005, 2015, 2020, and 2023. We employ the unsupervised classification of Landsat satellite imagery to examine changes in land cover and land use patterns. The data sourced from Landsat satellites: 4 (TM) from 2000, Landsat 7 (ETM+) from 2005 to 2010,

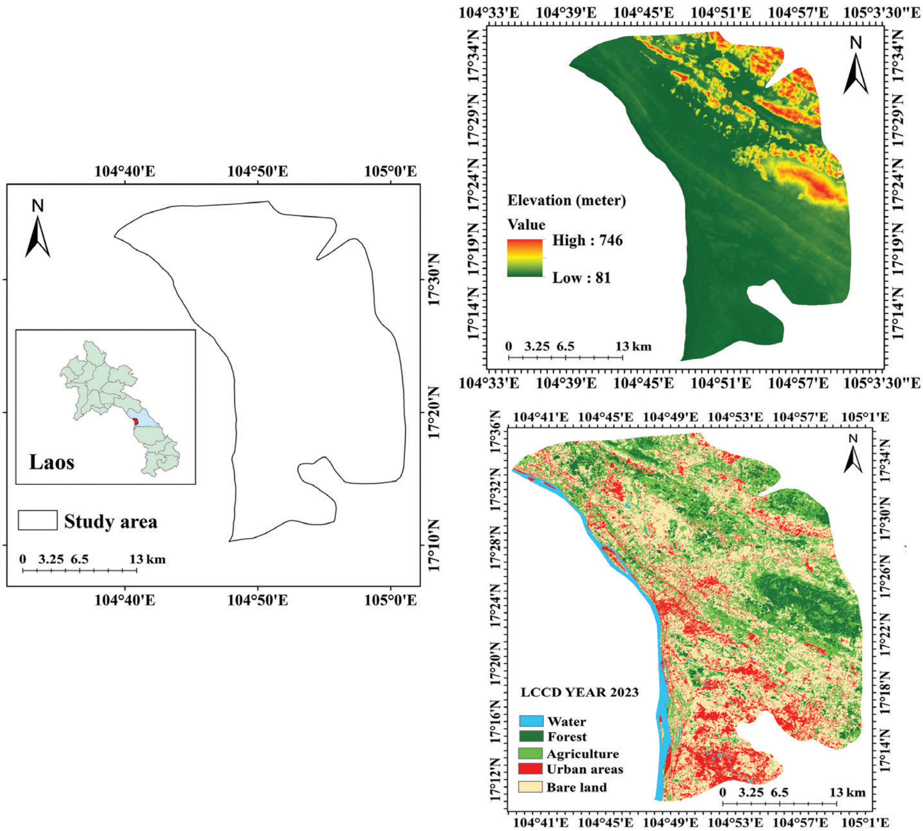

Figure 1. Map overview of the study area in Laos: Elevation and land cover change detection in 2023.

Table 1. Summary data collection.

Satellite	Sensor	Year(s) used	Spatial resolution	Temporal resolution	Data type
MODIS	Terra/Aqua	2000, 2015, 2020, 2023	1 km (LST)	Daily	Surface reflectance, LST
Landsat 4	TM	2000	30 m	16 days	Surface reflectance
Landsat 7	ETM+	2000, 2015, 2020	30 m	16 days	Surface reflectance, LST
Landsat 8	OLI/TIRS	2020, 2023	30 m (OLI), 100 m (TIRS)	16 days	Surface reflectance, LST
Landsat 9	OLI/TIRS	2021, 2023	30 m (OLI), 100 m (TIRS)	16 days	Surface reflectance, LST

Landsat 8 (OLI/TIRS) from 2015 to 2020, and Landsat 9 (OLI/TIRS) from 2023, maintaining a 30 m resolution for OLI and 100 m for TIRS, with the same 16-day revisit period.

We calculate the linear correlation coefficient (*LCCD*), which measures the linear relationship between the two variables, *x* and *y*. This metric is critical for analyzing the strength and direction of relationships between variables, helping to make informed decisions and improve research findings. The correlation formula used was Eq. 1.

$$LCCD = \frac{\sum_{i=1}^{n}(x_i - x)(y_i - y)}{\sqrt{\sum_{i=1}^{n}(x_i - x)^2 \sum_{i=1}^{n}(y_i - y)^2}}, \tag{1}$$

where *LCCD* is the Land Cover Change Cetection, x_i and y_i The individual data points for *LCCD* and *LST*. *x* and *y*: The means values of the *LCCD* and *LST* data. *n*: The number of data points in set. (x_i, y_i): The coordinates of the data points in the set. *x*: The mean value of the *x*-value of the data point. *y*: The mean value *y*-value of the data point.

To calculate the percentage change in *LCCD* by dividing the difference between two measurements by the $LCCD_{2000}$ measurement and then multiplying the result by 100. The formula employed was Eq 2.

$$LCCD = \frac{LCCD_{2023} - LCCD_{2000}}{LCCD_{2000}} \times 100, \tag{2}$$

where $LCCD_{2023}$ represented the *LCCD* measurement in 2023 and $LCCD_{2000}$ represented the *LCCD* measurement in 2000.

LST is crucial for environmental and climate studies as it influences processes such as temperature transfer and ecosystem dynamics. The MODIS on the Terra and Aqua satellites provides data to assess *LST* over specific spectral bands, which is essential for climate monitoring, agricultural management, and urban heat island research. To convert the raw satellite measurements into meaningful temperature values in degrees Celsius, we use special formulas to determine accurate *LST* values. We utilized Eqs. 3 and 4.

$$LST\_day\_1km = (LST\_day\_1km \times 0.02) - 273.15, \tag{3}$$

where the *LST_Day_1km* band, which is derived from the MODIS Land Surface Temperature products, provides the daytime land surface temperature in Kelvin, which is indicative of Earth's thermal infrared radiation. This formula converts the scaled digital values to Celsius.

$$LST\_night\_1km = Band6 * 0.02 + 273.15, \tag{4}$$

where *Band*6 is used to calculate nighttime *LST* from satellite data, specifically from the MODIS sensor. *Band*6 corresponds to the thermal infrared wavelengths that are critical for detecting surface temperature variations. A scaling factor of 0.02 is applied to convert raw digital data to Kelvin, while an offset of 273.15 is used to convert the temperature from Kelvin to Celsius.

4. Results

4.1. Dynamics of land use transitions

Over the past twenty-three years, the land cover changes demonstrate massive-scale geographical categories with maximum and minimum variations in the Thakhek district of Lao PDR. The results are a quantitative summary of the dynamics of the land use transitions from 2000 to 2023, as shown in Fig. 2. In 2000, forests and agriculture dominated the landscape, with minimal urban areas present. Forest cover was extensive, indicating less human intervention. The distribution of bare land was sparse, and water bodies remained intact. Agriculture and urban areas replaced some forest areas in 2005, especially those near water bodies. Urban expansion has slightly increased in the red regions, indicating that urbanization is beginning to take root in certain areas. In 2010, urban areas continued to expand, encroaching upon forested and agricultural land. Deforestation was noticeable, with some forest areas replaced by agriculture and bare land. A slight increase in bare land was visible, possibly due to urban development or agricultural land degradation. In 2015, urban areas showed considerable expansion, with forest loss continuing. Bare land areas increased, possibly due to soil degradation or human activities like mining or deforestation. In 2020, urban dominance was evident, with forest cover shrinking further, particularly in areas close to urban settlements. Agricultural land fluctuated over the years, indicating changes in land use priorities linked to population growth. In 2023, urban expansion is at its peak, taking over previously forested and agricultural areas.

Land use change is an essential aspect of environmental management and urban planning, with Tab. 2 illustrating the dynamic relationship between human activities and natural ecosystems. This study examines land use patterns from 2000 to 2023, focusing on five primary categories: forest, agriculture, water, urban area, and bare land. The data reveals significant changes in land cover due to factors like urbanization, agricultural expansion, and environmental management practices. The study found that the forest area declined to 1,190.92 km^2 by 2023, indicating deforestation or land conversion. Urban area increased from 879.08 km^2 in 2000 to 1,787.79 km^2 in 2023, indicating urban expansion and increased anthropogenic pressure.

Agricultural land use showed variability, peaking in 2010 at 3,490.70 km^2, before declining to 2,975.97 km^2 by 2023. The water category remained stable, with minor fluctuations, highlighting the importance of water bodies in the landscape.

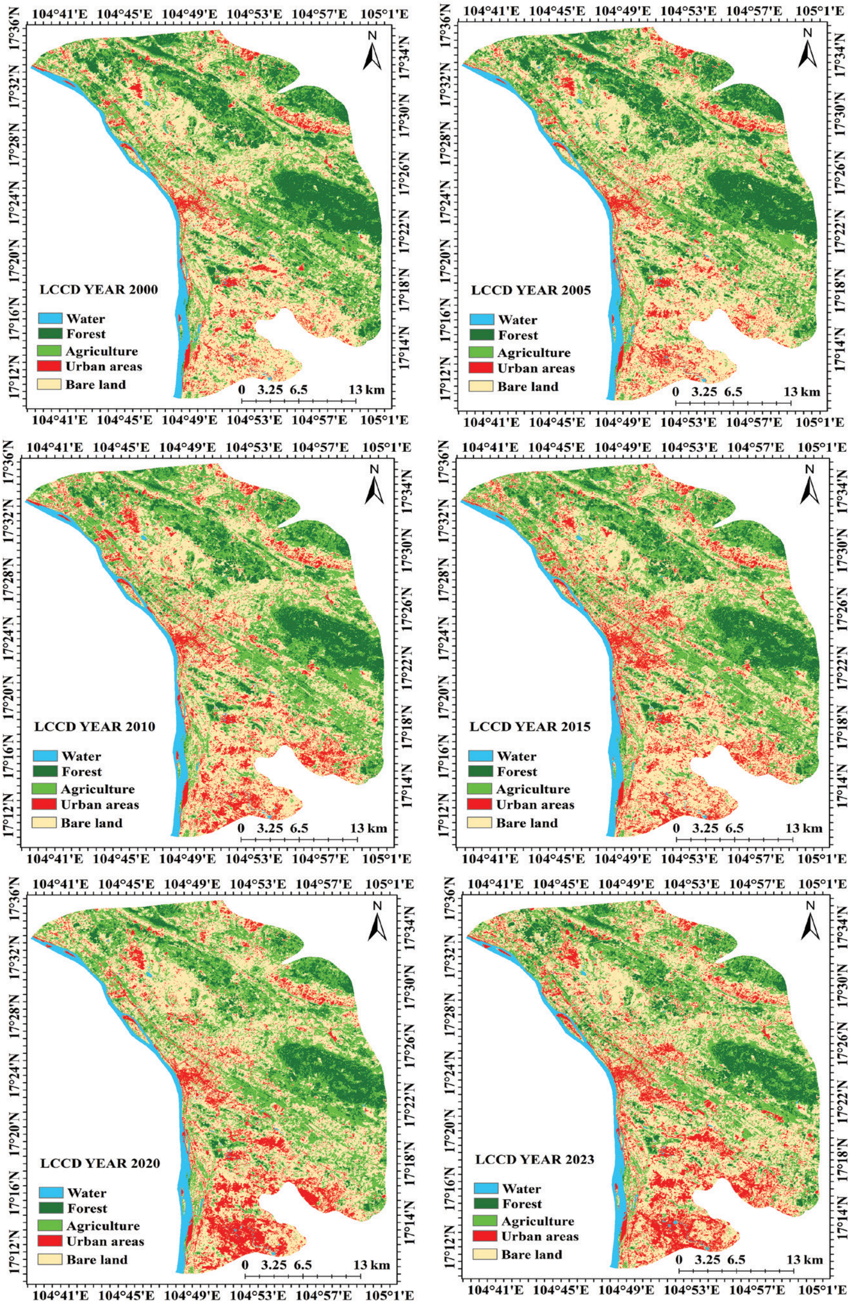

Figure 2. Dynamics of land cover change and urban expansion: A comprehensive analysis from 2000 to 2023.

Table 2. The quantitative summary of dynamics land use transitions and population data overview from 2000 to 2023.

Land use change

Year	Forest (km^2)	Agriculture (km^2)	Water (km^2)	Urban area (km^2)	Bare land (km^2)
2000	1,984.06	3,303.79	391.67	879.08	4,940.19
2005	1,933.10	3,019.66	398.6	986.3	5,161.13
2010	1,387.30	3,490.70	377.39	1,346.83	4,896.57
2015	1,344.91	3,409.54	393.9	1,436.27	4,914.17
2020	1,146.13	3,338.67	389.34	1,550.08	504.57
2023	1,190.92	2,975.97	389.78	1,787.79	515.33

Population data overview

Year	Population	Density (P/Km^2)	Yearly change	Yearly change (%)	Density change	Density change (%)	Urban population (%)	Urban Population
2000	79345	33	0	0	0	0	60	47607
2005	83957	33	4612	0.0581	0	0	58	48684
2010	85000	32	1043	0.0124	–1	–0.0303	56	47600
2015	90464	29	5464	0.0643	–3	–0.0938	54	48810
2020	94300	27	3836	0.0424	–2	–0.069	52	48886
2023	96485	25	2185	0.0232	–2	–0.0741	50	48243

However, the population trends from 2000 to 2023 focus on key indicators like total population, density, yearly changes, and urbanization rates. The data show a consistent upward trend in population, from 79,345 in 2000 to 96,485 in 2023. The population density decreased from 33 people per km^2 in 2000 to 25 people per km^2 in 2023, suggesting urban areas may be expanding outward to accommodate a growing population while reducing pressure on infrastructure. The analysis also shows fluctuations in yearly population change, with the urban population percentage increasing from 60% in 2000 to 50% by 2023, raising questions about the distribution of growth between urban and rural areas and its implications for land use and environmental sustainability.

The evolution of land cover types such as forest, agriculture, cultivated land, bare land, and water is evident in the percentage changes in land use from 2000 to 2023. Factors like urbanization, agricultural expansion, and climate change influence these changes, making understanding them crucial for effective environmental management, urban planning, and conservation. Each entry reflects the percentage change resulting from these changes. Figure 3 displays the result. The positive percentage changes in transitions such as "Water - Forest" (10.15%) and "Agriculture - Forest" (5.24%) indicate successful afforestation and reforestation efforts, highlighting a potential commitment to ecological restoration and biodiversity enhancement. Conversely, the negative shifts, such as "Forest - Water" (–9.34%) and "Bare Land – Water" (–8.89%), indicate significant losses of forested land that may impact local ecosystems, including habitat degradation

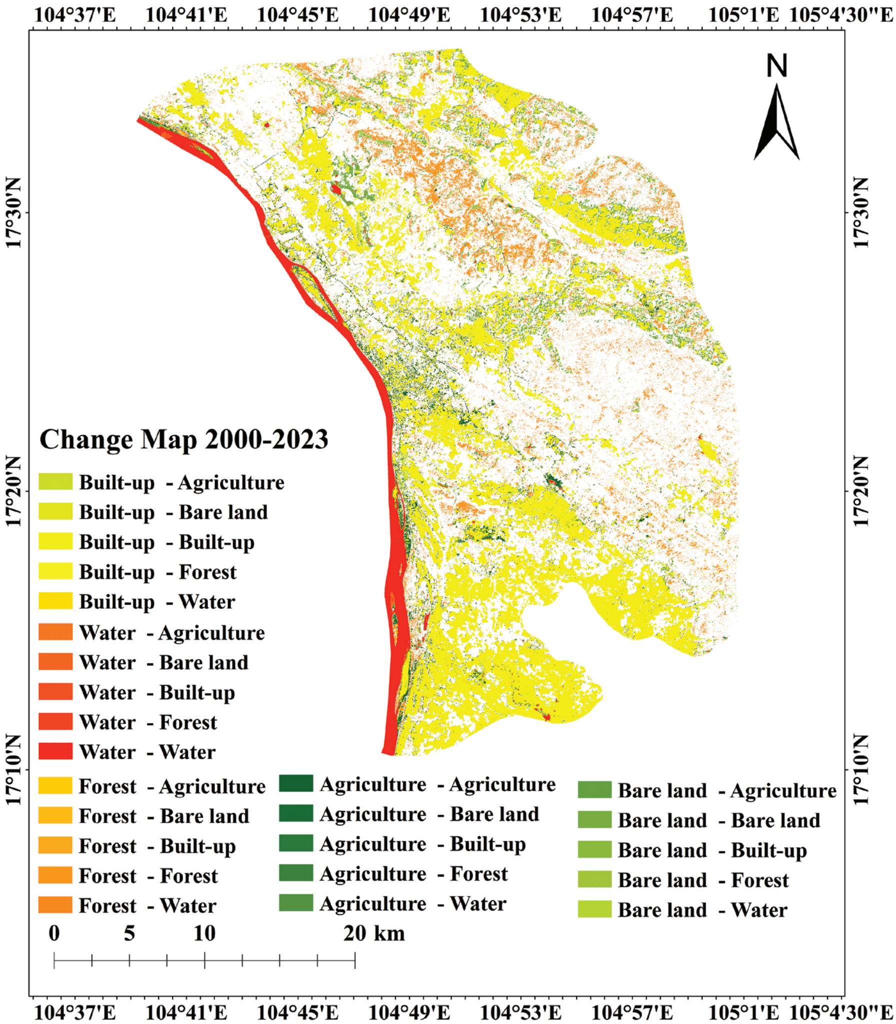

Figure 3. Dynamics of land use change: A comprehensive analysis (2000–2023).

and increased susceptibility to erosion. These shifts may also reflect broader trends related to water management and land reclamation practices that prioritize agricultural or urban development over natural landscapes. The transitions affecting built-up areas present a complex picture. For example, "Built-up - Agriculture" (–0.94%) indicates a slight reduction in agricultural land due to urban expansion, while the positive change in "Built-up - Built-up" (0.12%) indicates continued urban development. This data highlights the challenges faced by policymakers in balancing the need for development with the preservation of agricultural land and natural habitats.

Land use dynamics are essential for comprehending biological and environmental transformations within a region. Figure 4 analyzes the changes in land use categories—Forest, Agricultural, Urban, and Bare Land—over twenty years, from 2000 to 2023. The analysis highlights the substantial changes in land distribution and the effects of urbanization and environmental protection. In 2000, land use distribution indicated an increase in forest (39.7%) and agricultural (36.3%) regions, while urban areas (12.5%) and bare land (11.5%) represented a slightly smaller percentage. This equitable distribution signifies an area primarily defined by natural ecosystems and agricultural activities. By 2005, the urban area increased to 16.3%, indicating initial signs of urban expansion, while forest and agricultural areas decreased very little to 36.7% and 33.0%, respectively. Bare land experienced an increase of 14.0%, indicating a possibility of degradation or conversion. In 2010, the urban area expanded to 19.8%, while the forest area declined to 32.6%, signifying a transition toward urban land utilization. Bare land increased to 16.8%, highlighting persistent environmental change. The trend continued into 2015, with the urban area increasing to 23.4% and the forest area declining to 28.5%. Bare land increased to 21.0%, indicating a significant increase in areas with reduced vegetation. By 2020, the urban area reached a peak of 30.6%, demonstrating the increasing rate of urbanization. The forested area decreased to 25.3%, but bare land was constant at 21.0%. The latest data from 2023 indicates that the urban area has reached its peak at 36.5%,

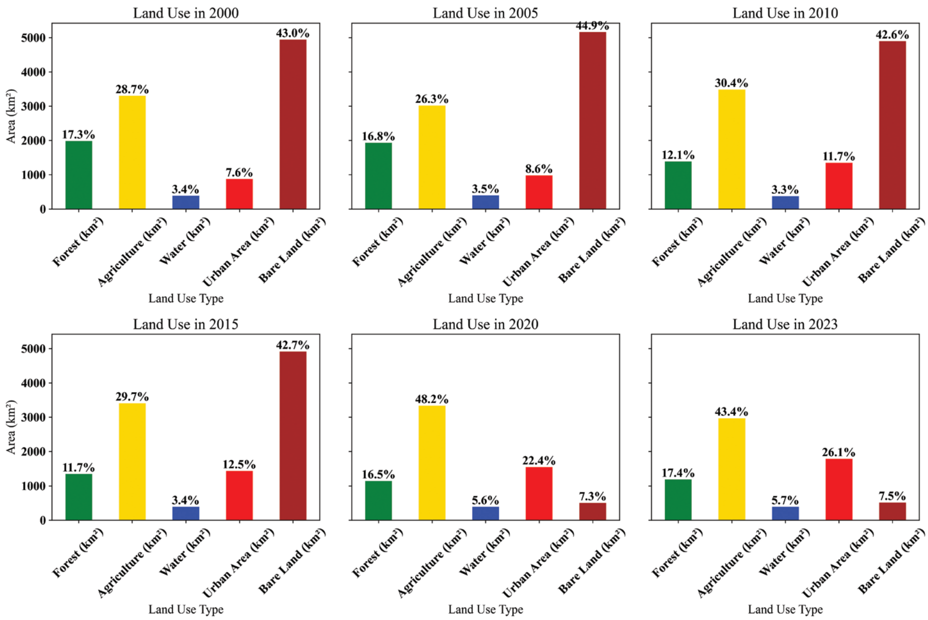

Figure 4. Total areas change for each class from 2000 to 2023.

Table 3. The quantitative summary of results land cover change detection.

Land use change 2000–2010				
Land use type	2000 (km²)	2010 (km²)	Change (km²)	Percentage Change
Forest	1984.06	1387.3	–596.76	↓ 30.1%
Agriculture	3303.79	3490.7	186.91	↑ 5.6%
Water	391.67	377.39	–14.28	↓ 3.6%
Urban area	879.08	1346.83	467.75	↑ 53.3%
Bare land	4940.19	4896.57	–43.62	↓ 0.9%
Land use change 2010–2023				
Land use type	2010 (km²)	2023 (km²)	Change (km²)	Percentage change
Forest	1387.3	1190.92	–196.38	↓ 14.2%
Agriculture	3490.7	2975.97	–514.73	↓ 14.7%
Water	377.39	389.78	12.39	↑ 3.8%
Urban area	1346.83	1787.79	440.96	↑ 32.6%
Bare land	4896.57	515.33	66.76	↑ 5.3%

while the forest area has significantly declined to 20.1%. The percentage of bare land increased to 42.6%, signifying a significant change in land use patterns and raising concerns about environmental sustainability.

Table 3 provides a comprehensive examination of land use change in specific regions from 2000 to 2010 and from 2010 to 2023, highlighting the variations between different land cover categories, including forest, agriculture, water bodies, urban areas, and wasteland. They indicate the area change for each category at the beginning and end of the period. Between 2000 and 2010, the forest area decreased significantly, from 1984.06 km² to 1387.30 km², a decrease of 30.1%. The agricultural area increased only slightly, from 3303.79 km² to 3490.70 km², which corresponds to an increase of 5.6%. The water area decreased only slightly from 391.67 km² to 377.39 km², which corresponds to a decrease of 3.6%. The urban area increased considerably, from 879.08 km² to 1346.83 km², which corresponds to an increase of 53.3%. The bare area decreased slightly from 4940.19 km² to 4896.57 km², which corresponds to a decrease of 0.9%. From 2010 to 2023, the forest area increased only slightly, from 1387.30 km² to 1190.92 km², which corresponds to a decrease of 14.2%. The area used for agriculture decreased from 3490.70 km² to 2975.97 km², which corresponds to a decrease of 14.7%. The water area remained constant with a small increase from 377.39 km² to 389.78 km², which corresponds to an increase of 3.8%. The urban area grew from 1346.83 km² to 1787.79 km² and from 4896.57 km² to 515.33 km², an increase of 5.3%.

4.2. Land surface temperature trends

To understand the daily mean *LST* of MODIS, we analyze the relationship between daytime and nighttime temperatures, which illustrates a fairly stable pattern over several years, with some fluctuations attributable to changes in

Table 4. Relationship between nighttime and daytime temperature changes.

Year	Nighttime Mean	Nighttime Max	Nighttime Min	Nighttime 25%	Nighttime 50%	Nighttime 75%	Nighttime Std Dev
2000	20	26	14	17	20	23	3.08
2015	22	26	12	21	23	25	3.13
2020	22	27	15	20	23	25	3.27
2023	23	28	14	22	24	25	3.29

Year	Daytime Mean	Daytime Max	Daytime Min	Daytime 25%	Daytime 50%	Daytime 75%	Daytime Std Dev
2000	28	30	24	28	28	29	1.26
2015	32	42	26	29	31	33	3.77
2020	30	32	26	28	30	31	1.85
2023	32	42	24	29	31	33	4.01

atmospheric conditions or shifts in land cover dynamics and only minor variations observed at night. The daytime and nighttime temperature fluctuations have a significant impact on both human activities and natural ecosystems. The results as shown in Tab. 4. The average nighttime and daytime temperatures of the areas in 2000 ranged from 17 °C to 28 °C for 25% of the areas, and from 20 °C to 28 °C for 50% of the areas, and from 23 °C to 29 °C for 75% of the areas. In comparison, the standard deviation is 3.08 and 1.26. Nevertheless, In 2015 the average temperature range 21 °C to 29 °C for 25% of the areas, from 23 °C to 31 °C for 50% of the areas, from 25 °C to 33 °C for 75% of the areas. In comparison, the standard deviation is 3.13 and 3.77. However, in 2020 the average temperature ranges from 20 °C to 28 °C for 25% of the areas, from 23 °C to 30 °C for 50% of the areas, and from 25 °C to 31 °C for 75% of the areas. In comparison, the standard deviation is 3.27 and 1.85. However, in 2023 the average temperature ranges from 22 °C to 29 °C for 25% of the areas, and from 24 °C to 31 °C for 50% of the areas, and from 25 °C to 33 °C for 75% of the areas. In comparison, the standard deviation is 3.29 to 4.01.

The results illustrate the complex interactions of the temperature change between 2000 and 2023, as shown in Fig. 5. illustrates Modis a relationship between temperature change during the daytime and at nighttime. In 2000, the observed nocturnal variation was between 14 °C and 19 °C, while daytime temperature was between 28 °C and 29 °C. In contrast, in 2015 according to the validation results, the accuracy of daytime around 31 °C and 42 °C, when compared to daytime from 2000, there are very high, while the nighttime temperature was 22 °C to 26 °C, while, the nighttime was between 22 °C to 25 °C, there are similar in 2000, however, both the daytime and nighttime temperatures continue to fluctuate. Natural climate change may have affected the daytime temperature in 2020, which decreased from 29 °C to 31 °C, but the nighttime temperature, which was similar to 2015, was 22 °C to 26 °C. However, the tem-

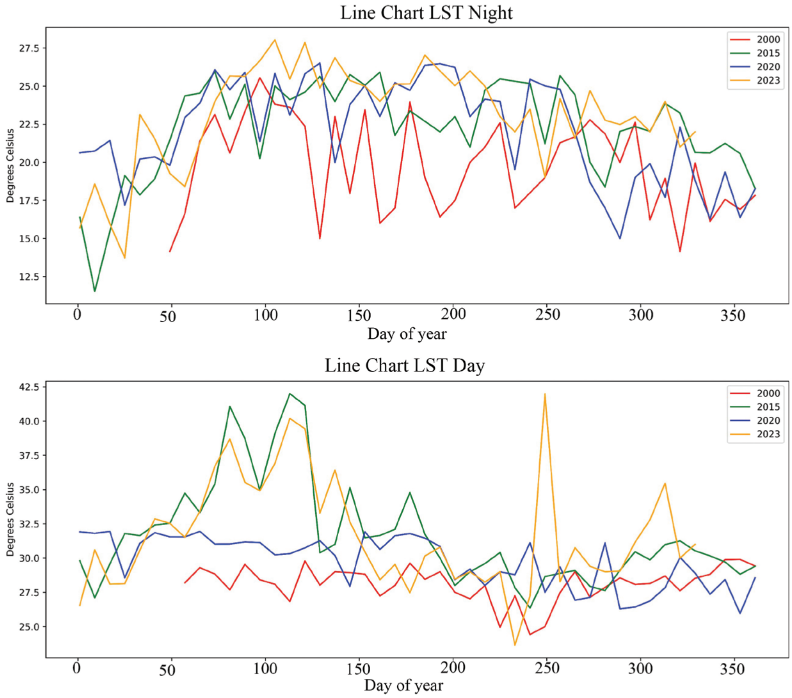

Figure 5. The temperature fluctuations over 23 years (2000–2023) highlight the intricate dynamics of daytime and nighttime land surface temperature (*LST*) trends for daytime and nighttime across the day of the year (0–350), where 0 corresponds to the beginning of the year (January 1) and 350 corresponds to December 16.

perature continues to fluctuate in 2023; the daytime temperature rises to between 31 °C and 42 °C. This is similar to the daytime temperature in 2015, which was between 23 °C and 28 °C. We also observed this trend in 2015. Various factors, such as urbanization and greenhouse gas emissions, could be responsible for this significant increase in daytime temperatures.

Furthermore, we also calculated a regression of daytime and nighttime to clarify and understand the temperature change. The results of a comparative analysis regression of *LST* were performed as shown in Fig. 6. In daytime and nighttime from 2000 to 2023 the relationship between the temperature of daytime and nighttime there is significantly scattered, the result regression in 2000 shows a negative slope of –0.2261 and a positive intercept of 26.0954. The positive *R*-squared value of 0.0086. Additionally, the positive *P*-value indicates a statistical significance of 0.5700. In 2015, we observed a significant positive slope of 0.2841 and a positive intercept of 13.2418. The significantly positive *R*-squared value of 0.1168 and the significantly positive *P*-value of 0.0201 indicate statistical significance. In 2020 was similar, as indicated positive a slope of 0.8622, but

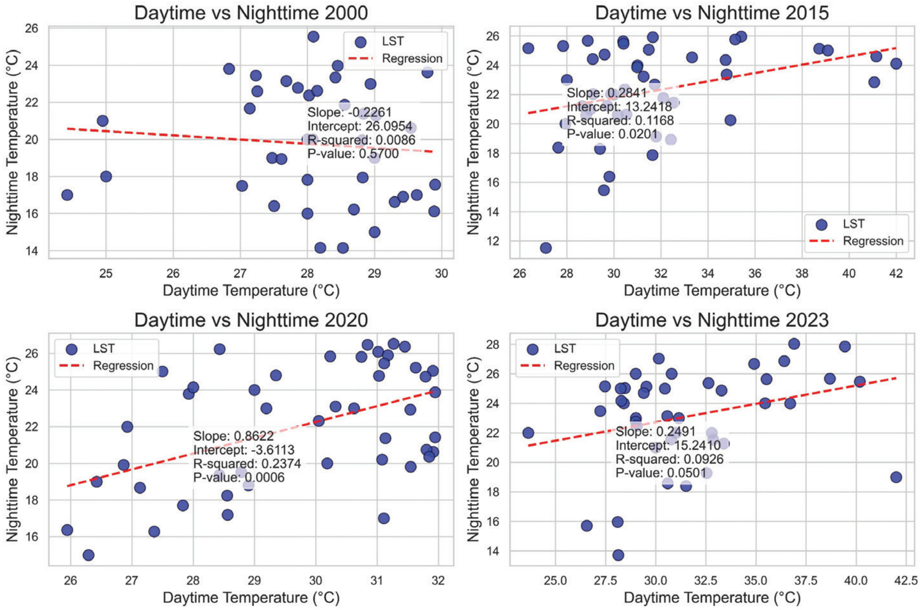

Figure 6. Density scatter point of daily mean daytime and nighttime temperature estimate with multiple linear regression.

different a negative intercept of –3.6113, In addition, The positive R-squared value of 0.2374. The significant positive *P*-value assesses the statistical significance of 0.0006. and the result in 2023 also had a similar result in 2015, but a different positive intercept value of 15.2410, and a positive slope of 0.2491, The positive *R*-squared of 0.0926, and the positive *P*-value assesses statistical significance of 0.0501.

Additionally, we analyzed histograms and found that an increase in the number of valid daytime and nighttime data used for multiple linear regression leads to improved accuracy in estimating the daily average daytime and nighttime temperatures. Figure 7 illustrates the nighttime temperatures in 2000. The histogram exhibits an area between 22.5 °C and 25.5 °C, accompanied by a relatively normal distribution curve that signifies moderate nighttime temperatures. The temperature distribution peaks at 28 °C and 31 °C, exhibiting a moderate dispersion and following a normal distribution during the day. In 2015, nighttime temperatures exhibited a small increase, ranging between 23.5 °C and 26.5 °C. Daytime temperatures have increased, with a maximum of around 30 °C to 33 °C, indicating a trend of temperature rise. In 2020, the nighttime temperatures showed significant warming, with the highest temperature fluctuating between 24.5 °C and 27.5 °C, suggesting a wider distribution. The temperature ranges are continuing to increase, reaching an average of approximately 32 °C to 35 °C dur-

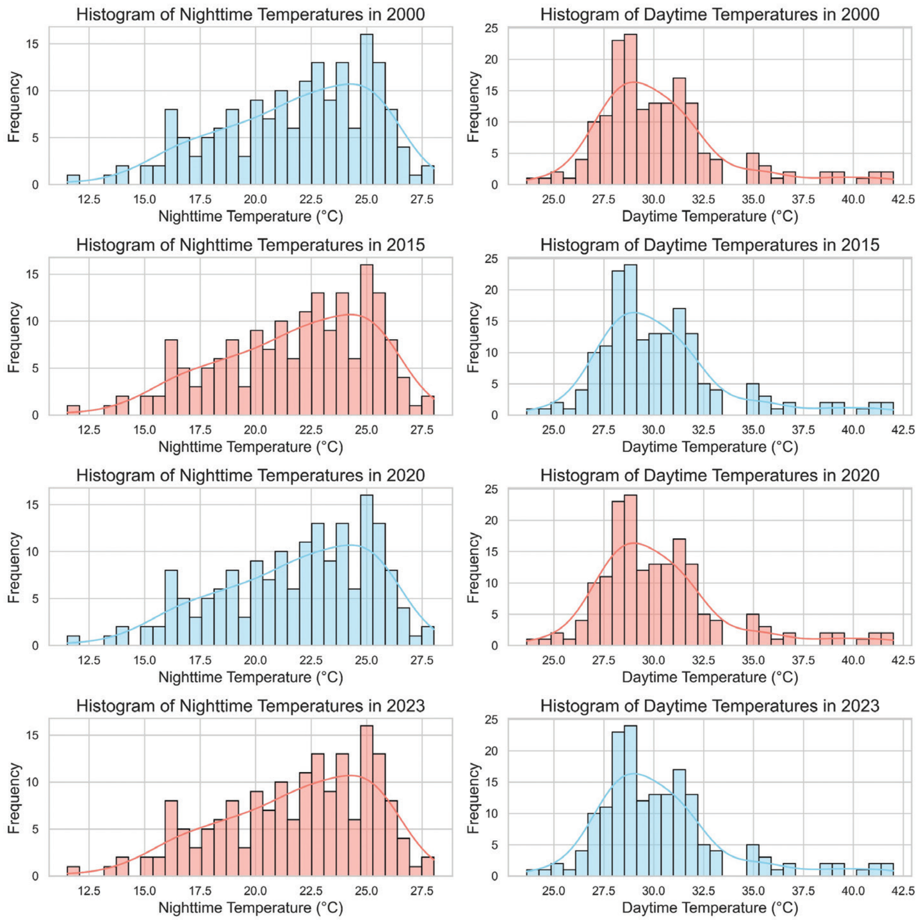

Figure 7. Histogram daytime and nighttime temperature to estimate the frequency daily mean in a site of 350 LST analysis via the multiple regression method.

ing the day, which signifies considerable warming. In 2023, nighttime temperatures reached their highest levels recorded, ranging between 25.5 °C and 27.5 °C, demonstrating the broadest distribution and indicating a significant warming trend. Daytime temperatures reached a maximum of between 33.5 °C and 37.5 °C, indicating a notable increase in comparison with previous years.

4.3. Land surface temperature trends and variability affect the environment and humans

LCCD and *LST* are important indicators of environmental change and its impact on ecosystems and human activities. As shown in Tab. 5, *LST* is higher in urban areas between 2000 and 2023 due to impermeable surfaces, such as

Table 5. Land cover change detection and land surface temperature.

Year	Forest (km^2)	Agri-culture (km^2)	Water (km^2)	Urban area (km^2)	Bare land (km^2)	LST Min	LST Max	LST Range	LST Mean	LST Std
2000	1984.06	3303.79	391.67	879.08	4940.19	24.32	33.3	8.98	27.17	0.68
2005	1933.1	3019.66	398.6	986.3	5161.13	21.76	31.11	9.35	26.03	1.13
2010	1387.3	3490.7	377.39	1346.83	4896.57	19.48	29.52	10.03	25.03	1.13
2015	1344.91	3409.54	393.9	1436.27	4914.17	21.76	31.22	9.46	26.8	0.93
2020	1146.13	3338.67	389.34	1550.08	504.57	19.29	29.34	10.05	24.12	1.09
2023	1190.92	2975.97	389.78	1787.79	515.33	31.01	42.16	18.15	28.89	2.14

concrete and asphalt, that absorb and store heat. This phenomenon, known as the urban heat island effect, leads to increased temperatures in urban areas both during the day and at night. The conversion of other land cover types is further evidence of the impact of land use change on *LST*. The conversion of forests, agricultural land, and vegetated land to urban areas changes their thermal characteristics. Forests, for example, generally absorb less solar radiation and have a cooler surface temperature due to their vegetation cover and evaporative cooling. The data from the table shows a decrease in forest area from 1984.06 km^2 in 2000 to 1146.13 km^2 in 2020, which correlates with an increase in *LST* from 24.32 °C to 19.29 °C, respectively. Conversely, impervious surfaces in urban areas absorb more solar energy, resulting in higher LST. The area of urban areas increased from 879.08 km^2 in 2000 to 1787.79 km^2 in 2023, contributing significantly to the warming trend observed in the region, with the *LST* increasing from 33.3 °C in 2000 to 42.16 °C in 2023. This transformation not only reduces the cooling effect of green spaces but also contributes to an overall warming of the region. The data in the table illustrates this dynamic, with decreasing forest areas and increasing urban areas correlating with higher LST. Understanding these land use changes and their impact on *LST* is critical to developing strategies to mitigate urban heat islands through urban planning and the creation of green infrastructure such as parks and green roofs, which can help cool urban environments and reduce the negative impacts of *LST* on human health and well-being.

The summary of the *OLS* (Ordinary Least Squares) regression analysis illustrates the relationships between the independent variables and the dependent variable, the *LST* mean. Table 6 shows the model's R-squared value of 0.956, indicating a strong fit, with the independent variables accounting for approximately 95.6% of the variability in the *LST* mean. The adjusted R-squared value of 0.778 accounts for the number of predictors and explains approximately 77.8% of the variability after adjusting for model complexity. We test the significance of the model using the F-statistic of 5.384, and the p-value of 0.311 indicates that the overall model does not show statistical significance at conventional levels. The log-likelihood of –1.741 measures model fit, while the Akaike Information Crite-

Table 6. The Ordinary Least Squares (OLS).

Dep. variable:	*LST* mean	R-squared:	0.956			
Model:	OLS	Adj. R-squared:	0.778			
Method:	Least squares	F-statistic:	5.384			
No. observations:	6	*AIC*:	13.48			
Df Residuals:	1	*BIC*:	12.44			
Df Model:	4	Covariance type:	nonrobust			
Variable	coef	Std. error	t	$P>\|t\|$	[0.025	0.975]
Constant Term	–86.7114	38.335	–2.262	0.265	–573.8	400.377
Forest (km²)	0.0288	0.009	3.348	0.185	–0.081	0.138
Agriculture (km²)	0.0094	0.005	1.918	0.306	–0.053	0.072
Urban Area (km²)	0.0298	0.008	3.601	0.172	–0.075	0.135
Bare Land (km²)	–0.0002	0	-0.533	0.688	–0.004	0.004
Omnibus:		nan	Durbin-Watson:		2.709	
Prob (Omnibus):		nan	Jarque-Bera (JB):		0.046	
Skew:		–0.169	Prob (JB):		0.977	
Kurtosis:		2.738	Cond. No.		6.40E+05	

rion (*AIC*) of 13.48 and the Bayesian Information Criterion (*BIC*) of 12.44 indicate potential for model refinement. The coefficient analysis shows a positive relationship between forest area and the *LST* mean. The correlation between agricultural area and mean land surface temperature is similarly non-statistically significant. The correlation with urban areas is also not statistically significant. The adverse correlation with bare land is minimal. The residual diagnosis shows a strong model, as shown by a Durbin-Watson statistic of 2.709 and a Jarque-Bera test result of 0.046, which means that the residuals are spread out normally.

Figure 8 illustrates the correlation between mean *LST* and significant land cover features, as well as the temporal trend from 2000 to 2023 in Thakhek, Laos. Figure 8a illustrates an increase in mean *LST* over time, increasing from approximately 26 °C in 2000 to 28 °C in 2023. This highlights a warming trend possibly influenced by changes in land cover and urbanization. Figure 8b illustrates the relationship between forest area and *LST*. The forest area decreased from 2,000 km² to 1,200 km² during the study period, indicating a slight positive relationship between forest loss and increasing *LST* values. Figure 8c shows the correlation between urban area and *LST*. Urban areas increased from around 1,000 km² in 2000 to 1,800 km² in 2023, demonstrating a significant positive link with elevated *LST*. This illustrates the impact of the urban heat island effect as a significant contributor to regional temperature elevations. Fig. 8d depicts the correlation between barren land and *LST*. The expanse of barren terrain surged significantly from 1,000 km² to almost 5,000 km². Nonetheless, the association with *LST* exhibited considerable variability, indicating that the influence of barren land on temperature trends is less strong than that of urban and forest changes.

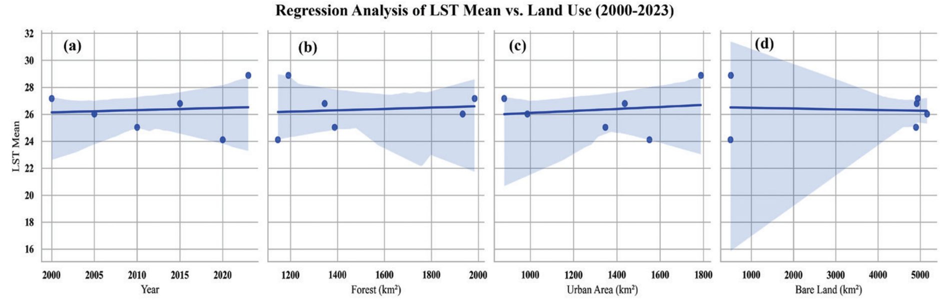

Figure 8. Scatter plots of land surface temperature mean against land use variables over time.

4.4. Correlation relationship between LCCD and LST

To analyze the correlation relationship between *LCCD* and *LST*. Figure 9 illustrates this result clearly. Through a careful evaluation of correlation matrices. We have uncovered subtle relationships that shed light on the complicated interaction; the correlation analysis between the *LCCD* and *LST* over time between 2000, 2005, 2010, 2015, 2020, and 2023 is computed. The correlation illustrates relationships between *LCCD* and *LST* that vary in strength and direction over time. The relationship between the *LCCD* and *LST* within the same year exhibits the highest degree of association, suggesting direct effects on the land surface temperature. The presence of weaker correlations across different years suggests indirect effects that could be influenced by factors not considered in this analysis.

As revealed by the correlation matrix in 2000, there was a significant positive connection (0.67) between *LCCD* in 2000 and 2023. This finding indicates a significant amount of continuity in *LCCD* patterns over time. However, we observed a notable positive correlation (0.67) between *LCCD* in 2000 and *LST* in 2023. Conversely, we identified a slight negative correlation (–0.50) between *LCCD* in 2000 and *LST* in 2010, which suggests a marginally negative relationship. In 2005, the correlation between *LCCD* and *LST* was negative (–0.51), reflecting a relatively stronger negative association for that year. The correlation between *LCCD* in 2005 and *LST* in 2010 was also slightly negative (–0.61), suggesting inconsistencies in land cover and surface temperature during that time. The findings from 2015 demonstrate a notable positive correlation (0.74) between *LCCD* in 2015 and *LST* in 2020, indicating regular and persistent patterns of land cover change during this period. A significant positive correlation (0.15) was also established between *LCCD* and *LST* within the same year, 2015. However, the relationship between *LST* in 2015 and *LCCD* in 2020 exhibited small negative correlations (–0.08), indicating some fluctuations. We observed a significant positive correlation in 2020. However, the result in 2020 revealed a notable negative correlation (–0.66) between *LCCD* and *LST*, indicating a relationship between these two factors in the same year. In contrast, the *LCCD* in 2020 and

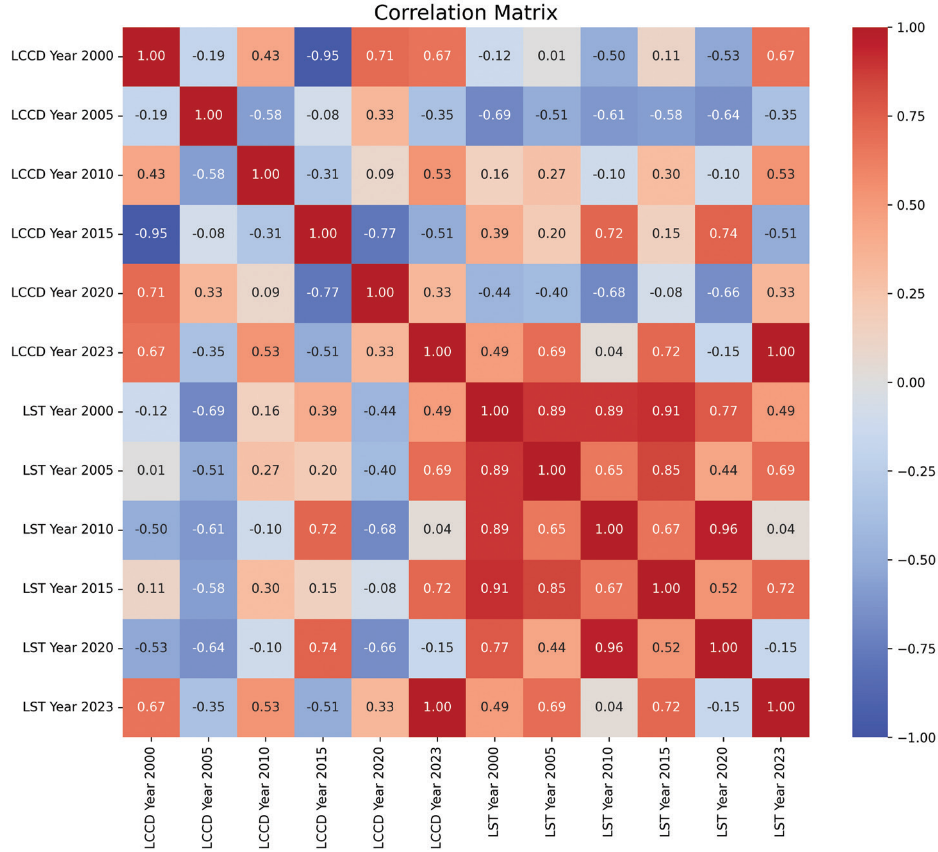

Figure 9. Correlation matrix relationship between *LCCD* and *LST*.

LST in 2023 there is a moderate positive correlation (0.33), which indicates a moderate positive correlation between these two variables. In 2023 the relationship between *LCCD* and *LST* illustrated a significant negative correlation (–0.09). The result of a correlation between *LST* in 2023 and 2015, as indicated, the relationship between the variables and correlation coefficient is a strong positive (0.72). The correlation patterns show that the associations between *LCCD* and *LST* vary in intensity and direction over time.

5. Discussion

The study examines the relationship between Land Cover Change Dynamics (*LCCD*) and Land Surface Temperature (*LST*) from 2000 to 2023, revealing significant trends and shifts in these relationships due to climatic conditions, human activities, and land management practices.

The significant positive correlation (0.84) between *LCCD* in 2000 and *LST* in 2023 signifies a consistent trend in land cover dynamics, underscoring the enduring impact of land cover changes over two decades. This finding corresponds with the research conducted by Addae et al. (2019), which demonstrated a comparable continuity in land use patterns and their effects on urban areas in Ghana. The modest negative correlation (–0.52) between *LCCD* and *LST* in 2000 indicates a developing link in which changes in land cover may not have completely impacted surface temperatures. In 2015, the strong positive correlation (0.96) between *LCCD* and *LST* indicates a significant relationship between changes in land cover and temperature, driven by increased urbanization and agricultural efforts throughout this period. This corresponds to Ashwini et al. (2022) research, which revealed the same trends in Northeast India. The positive correlation (0.47) between *LCCD* and LST in 2015 highlights the direct impact of land cover changes on local temperatures, emphasizing the relationship between human activities and the environment. The slight negative correlation (–0.61) between *LCCD* in 2015 and LST in 2020 suggests a decreasing impact of land cover changes over time. Changing land management and overall climatic patterns may contribute to this relationship's complexity. This finding aligns with the research conducted by Azadi et al. (2021), which investigated the effects of agricultural land conversion on climate change, emphasizing the resilience of landscapes to changing environments.

Between 2020 and 2023, the findings indicate significant changes in the relationship between *LCCD* and *LST*. The strong positive relationship (0.83) between *LCCD* and *LST* in 2020 shows that land cover changes are still being impacted over this time, which is similar to Hassan Edan et al. (2021) results. The moderate negative correlation (–0.11) between *LCCD* in 2020 and *LST* in 2023 suggests a decreasing link over time, indicating potential changes in land management and the landscape. In 2023, an observed negative correlation (–0.09) between *LCCD* and *LST* shows a decoupling of both variables. This may be a consequence of increasing urbanization, afforestation, or land manage-ment strategies that change the landscape without directly affecting surface temperatures. The results of Ru et al. (2022) and Güneralp et al. (2020) support this theory. They investigated the effects of changing land use and land cover on temperature at different locations. The decreasing correlation over time illustrates the importance of changing management strategies to cope with changing environmental conditions.

The study highlights the importance of understanding the relationship between land cover change (*LCCD*) and local temperature change (*LST*) for environmental management and policy. It suggests that incorporating knowledge of land cover change into urban planning and agricultural policy can contribute to the development of sustainable and resilient landscapes. The shifts in correlation patterns also highlight the need for adaptive management practices, such as afforestation, reforestation, and sustainable agriculture, to improve landscape resilience and manage the effects of temperature over time.

The study on land cover dynamics and land surface temperature from 2000 to 2023 provides important insights but also has its limitations. Because it relies on remote sensing data and the resolution of *LST* data, it may not fully capture microscale changes in land cover and their direct effects on temperature. The temporal scope of the study also limits its generalizability to other regions or climate zones. Further action should focus on the importance of sustainable prediction of forest change, water, agriculture, bare land, and urban areas. For proactive measures and policies to be implemented, we need to be able to predict land cover change with a high degree of accuracy. This also requires comprehensive land use planning strategies and the involvement of local communities in conservation and reforestation efforts to ensure mutual benefit and active participation in sustainable land use practices.

6. Conclusion

Over the past twenty-three years, the Thakhed district has experienced land cover change due to human activities, deforestation, afforestation and change in land surface temperature as a result of climate change. The result shows different spatial arrangements, exhibited erratic fluctuations, by a decrease in water bodies in 2015 and an increase in 2023. In 2015 there was an increase in bare land which is a direct effect of deforestation and a subsequent decrease in 2023 owing to government interventions. Forested areas experienced a substantial decrease due to anthropogenic activities, although positive regeneration was observed in 2023, expedited by restoration initiatives. Agricultural land showed diverse patterns, initially experiencing expansion and subsequently contracting as a result of environmental changes and urbanization. The urban areas experienced significant growth, fueled by increased in population and industrialization efforts.

Human activities, population growth, environmental shifts, and deforestation have all contributed to changes in land use, which have transformed forests into agricultural zones and urban areas. These changes have had a significant impact on land surface temperature. In addition, we also analyzed a relationship between land *LCCD* and *LST*, as shows both positive and negative correlations. The relationship between *LCCD* and *LST* is influenced by urbanization, deforestation, and climate change. Weaker correlations in different years indicate indirect effects that are influenced by additional variables and make the relationship between *LCCD* and *LST* in the region even more complex. These findings demonstrate the complex relationship between land use changes and temperature dynamics.

Credit authorship contribution statement – **Ketsana Phommavong**: Conceptualization, methodology, validation, writing – original draft, visualization, data curation, formal analysis. **Jianguo Yan**: Writing – review & editing, data curation, investigation.

Declaration of competing interest – The authors declare that they have no known competing financial interests or personal relationships that could have appeared to influence the work reported in this paper.

Data availability – Data will be available on reasonable request to the authors.

Funding – The open project of the Key Laboratory in Xinjiang Uygur Autonomous Region of China (2023D04058), Chinese Academy of Sciences Foundation of the young scholars of western (2020-XBQNXZ-019), and the National Natural Science Foundation of China (Grant No. 42241116) supports this project under. Jianguo Yan was funded by the 2022 Project of the Xinjiang Uygur Autonomous Region of China, specifically the Heaven Lake Talent Program.

Acknowledgements – We would like to express our gratitude to the Modis and Landsat science teams at NASA for providing the data that enables our research.

References

Addae, B. and Oppelt, N. (2019): Land-use/land-cover change analysis and urban growth modelling in the Greater Accra Metropolitan Area (GAMA), Ghana, *Urban Science*, **3**(1), Article 1, https://doi.org/10.3390/urbansci3010026.

Aram, F., García, E. H., Solgi, E. and Mansournia, S. (2019): Urban green space cooling effect in cities, *Heliyon*, **5**(4), https://doi.org/10.1016/j.heliyon.2019.e01339.

Ashwini, K. and Sil, B. S. (2022): Impacts of land use and land cover changes on land surface temperature over Cachar Region, Northeast India – A case study, *Sustainability*, **14**(21), https://doi.org/10.3390/su142114087.

Azadi, H., Taheri, F., Burkart, S., Mahmoudi, H., De Maeyer, P., and Witlox, F. (2021): Impact of agricultural land conversion on climate change. Environment, *Development and Sustainability*, **23**(3), 3187–3198, https://doi.org/10.1007/s10668-020-00712-2.

Bucała, A. (2014): The impact of human activities on land use and land cover changes and environmental processes in the Gorce Mountains (Western Polish Carpathians) in the past 50 years, *J. Environ. Manage.*, **138**, 4–14, https://doi.org/10.1016/j.jenvman.2014.01.036.

Cosslett, T. L. and Cosslett, P. D. (2018): The setting of mainland Southeast Asian countries: Cambodia, Laos, Thailand, and Vietnam, In: *Sustainable Development of Rice and Water Resources in Mainland Southeast Asia and Mekong River Basin*, edited by: Cosslett, T. L. and Cosslett, P. D. Springer, Singapore, pp. 5–27, https://doi.org/10.1007/978-981-10-5613-0_2.

Derdouri, A., Wang, R., Murayama, Y. and Osaragi, T. (2021): Understanding the links between LULC changes and SUHI in cities: Insights from two-decadal studies (2001–2020), *Remote Sens.*, **13**(18), https://doi.org/10.3390/rs13183654.

Gogoi, P. P., Vinoj, V., Swain, D., Roberts, G., Dash, J. and Tripathy, S. (2019): Land use and land cover change effect on surface temperature over Eastern India, *Sci. Rep.*, **9**(1), 8859, https://doi.org/10.1038/s41598-019-45213-z.

Güneralp, B., Reba, M., Hales, B. U., Wentz, E. A. and Seto, K. C. (2020): Trends in urban land expansion, density, and land transitions from 1970 to 2010: A global synthesis, *Environ. Res. Lett.*, **15**(4), 044015, https://doi.org/10.1088/1748-9326/ab6669.

Hassan Edan, M., Muhsen Maarouf, R. and Hasson, J. (2021): Predicting the impacts of land use/land cover change on land surface temperature using remote sensing approach in Al Kut, Iraq, *Phys. Chem. Earth*, **123**, 103012, https://doi.org/10.1016/j.pce.2021.103012.

Jin S., D., Ke, W., Yang, H. and Jia, G. Q. (2009): Spatio-temporal dynamics and evolution of land use change and landscape pattern in response to rapid urbanization, *Landscape Urban Plan.*, **92**(3–4), 187–198, https://doi.org/10.1016/j.landurbplan.2009.05.001.

José Maria Cardoso da, S., Prasad, S. and José Alexandre Felizola, D.-F. (2017): The impact of deforestation, urbanization, public investments, and agriculture on human welfare in the Brazilian Amazonia, *Land Use Policy*, **65**, 135–142, https://doi.org/10.1016/j.landusepol.2017.04.003.

Mahmood, R., Pielke, R. A., Hubbard, K. G., Niyogi, D., Bonan, G., Lawrence, P., McNider, R., McAlpine, C., Etter, A., Gameda, S., Qian, B., Carleton, A., Beltran-Przekurat, A., Chase, T., Quintanar, A. I., Adegoke, J. O., Vezhapparambu, S., Conner, G., Asefi, S., Sertel, E., Legates, D. R., Wu, Y., Hale, R., Frauenfeld, O. W., Watts, A., Shepherd, M., Mitra, C., Anantharaj, V. G., Fall, S., Lund, R., Treviño, A., Blanken, P., Du, J., Chang, H.-I., Leeper, R., Nair, U. S., Dobler, S., Deo, R. and Syktus, J. (2010): Impacts of land use/land cover change on climate and future research priorities, *B. Am. Meteorol. Soc.*, **91**(1), https://doi.org/10.1175/2009BAMS2769.1.

Ru, X., Song, H., Xia, H., Zhai, S., Wang, Y., Min, R., Zhang, H., and Qiao, L. (2022): Effects of land use and land cover change on temperature in summer over the Yellow River Basin, China, *Remote Sens.*, **14**(17), https://doi.org/10.3390/rs14174352.

Sruthi, S. and Mohammed, A. M. A. (2015): Agricultural drought analysis using the NDVI and land surface temperature data: A case study of Raichur District, *Aquat. Pr.*, **4**, 1258–1264, https://doi.org/10.1016/j.aqpro.2015.02.164.

Xu, S., Yang, K., Xu, Y., Zhu, Y., Luo, Y., Shang, C., Zhang, J., Zhang, Y., Gao, M. and Wu, C. (2021): Urban land surface temperature monitoring and surface thermal runoff pollution evaluation using UAV thermal remote sensing technology, *Sustainability*, **13**(20), https://doi.org/10.3390/su132011203.

SAŽETAK

Korištenje daljinskog očitavanja za praćenje promjena pokrova zemlje i kolebanja temperature površine zemlje u Laosu

Ketsana Phommavong i Jianguo Yan

Detekcija promjene zemljišnog pokrova (*LCCD*) ključna je za olakšavanje očuvanja okoliša i nastojanja održivog razvoja diljem svijeta. Ova studija ispituje odnos između LCCD i temperature površine zemlje (*LST*) u Thakheku, Laos, od 2000. do 2023. Procjenjujemo odnos između promjena u obrascima korištenja zemljišta i varijacija temperature površine zemlje (*LST*) koristeći Landsat-5, Landsat-8 i Skupovi podataka spektroradiometra umjerene rezolucije (MODIS). Naši rezultati ukazuju na značajno smanjenje šumskog područja, koje se smanjuje sa 46.912 km² u 2000. godini na 33.955 km² u 2023. godini, prvenstveno zbog ljudskih aktivnosti i brze urbanizacije. Istodobno se neplodna površina povećala na 515,33 km², dok se poljoprivredna površina značajno smanjila na 2.975,97 km². Promatrane *LST* vrijednosti pokazuju značajne promjene, u rasponu od 24 °C do 33 °C 2000. godine i proširenje na 20 °C do 41 °C 2023. godine, što ukazuje na opći porast temperature. Rezultati ilustriraju značajnu korelaciju između urbanog razvoja, rasta stanovništva i promjena zemljišnog pokrova, koje utječu na regionalne temperaturne trendove u Thakheku. Ovi rezultati naglašavaju hitnu potrebu za ciljanim istraživanjem i političkim mjerama koje kombiniraju razvoj i ekološku održivost i osiguravaju skladnu regionalnu budućnost.

Ključne riječi: promjena zemljišnog pokrova, temperatura površine zemlje, Laos, urbanizacija, daljinska detekcija

Corresponding authors' addresses: Ketsana Phommavong and Jianguo Yan, State Key Laboratory of Information Engineering in Surveying, Mapping and Remote Sensing, Wuhan University, Wuhan 430070, China; e-mail1: ketsana.pk@whu.edu.cn; e-mail2: jgyan@whu.edu.cn